# High Field $^{31}$P ENDOR of MnAlPO$_4$-20: Direct Evidence for Framework Substitution

**D. Arieli,[†] D. E. W. Vaughan,[‡] K. G. Strohmaier,[‡] and D. Goldfarb*[,†]**

*Contribution from the Department of Chemical Physics, Weizmann Institute of Science, Rehovot 76100, Israel, and Exxon Research and Engineering Company, Route 22 East, Annandale, New Jersey 08801*

*Received February 5, 1999. Revised Manuscript Received April 13, 1999*

**Abstract:** The incorporation of Mn(II) into framework sites in the aluminophosphate zeotype AlPO$_4$-20, an analog of sodalite, has been investigated using pulsed electron nuclear double resonance (ENDOR) spectroscopy at 95 GHz. The field sweep echo-detected EPR spectrum showed the presence of a single Mn(II) site with a $^{55}$Mn hyperfine coupling of 8.7 mT. ENDOR spectra, recorded using the Mims and Davies sequences, consist of an $^{27}$Al signal at the Larmor frequency and a $^{31}$P doublet corresponding to a hyperfine coupling of 8 MHz. The symmetry of the doublet about the $^{31}$P Larmor frequency indicates that it originates from the $M_S = \pm 1/2$ manifolds and that the interaction is primarily isotropic. The relatively large $^{31}$P hyperfine interaction and the weak interaction with $^{27}$Al provide unique and direct evidence for Mn(II) substitution of framework Al. X-band electron spin echo envelope modulation (ESEEM) measurements showed only signals at the $^{1}$H, $^{14}$N, $^{27}$Al, and $^{31}$P Larmor frequencies. The first two are due to weak dipolar interaction with the template molecules, while the others reflect interactions with the framework.

## Introduction

The aluminophosphate molecular sieves, AlPO$_4$-*n*, first reported by Wilson et al.,[1] are microporous zeotype materials with pore dimensions useful for adsorption and molecular sieving. Unlike lattices of typical zeolites their lattice is neutral, and they thus exhibit no ion-exchange ability or acidity. These, properties however, can be introduced by transition-metal (TM) ions substitution.[2] Various AlPO$_4$-*n* materials containing first series TM ions (MeAlPO$_4$-*n*), and exhibiting a wide range of compositions have been synthesized during the last two decades.[2−4] One of these ions, which was successfully incorporated into different AlPO$_4$-*n* structures and which showed some specific catalytic activity in hydrocarbon cracking is Mn-(II).[4]

Wilson et al.[3] have used the framework stoichiometry, provided by chemical analysis, the chemical purity of the doped phases, and the production of strong Brönsted acidity as evidences for framework substitution. Lattice distortions introduced by the chemical modification and the induction of ion-exchange character were also consistent with framework substitution.[2] These are, however, indirect evidences. Electronic spectroscopy in the UV−visible region is often applied for studying TM ions.[5] There, the d-d- and charge-transfer bands are used to follow valence changes and structural modifications of the zeolite.[6] Unfortunately, these are often insufficient for a detailed description of the TM local environment.

A direct evidence for framework substitution was obtained by $^{31}$P magic angle spinning (MAS) NMR of MgAlPO$_4$-20,[7] where insight into the ordering of Mg and Si in the framework was obtained from the presence of $^{31}$P lines with different chemical shifts. When paramagnetic metals are involved, use has been made of the paramagnetic shift effects[8] on the MAS spectra of $^{27}$Al and $^{31}$P in MnAlPO$_4$-5[9] and different CoAlPO$_4$-*n*.[10] In the latter, large isotropic shifts were observed.

The combination of conventional continuous wave (CW) EPR and various pulsed methods have often been used to probe the close environment of paramagnetic centers in zeotype materials. The X-band ($\nu_0 \approx 9$ GHz) CW EPR spectrum of Mn(II) in zeolites is usually centered at $g \approx 2$, and its spectral characteristics are determined, primarily, by the zero-field splitting (ZFS) and $^{55}$Mn(II) hyperfine parameters.[11] These parameters provide information on the symmetry and coordination number of the manganese ions.[12] However, a better insight into the Mn-(II) close chemical environment is provided by the superhyperfine interactions with neighboring magnetic nuclei. Such interactions are usually determined by the application of electron spin echo envelope modulation (ESEEM)[13−15] and electron

[†] Weizmann Institute of Science.

[‡] Exxon Research and Engineering Company.

(1) Wilson, S. T.; Lock, B. M.; Messina, C. A.; Cannan, T. R.; Flanigen, E. M. *J. Am. Chem. Soc.* **1982**, *104*, 1146−1147.

(2) Pyke, D. R.; Whitney, P.; Houghton, H. *Appl. Catal.* **1985**, *18*, 173−190.

(3) Flanigen, E. M.; Lok, B. M.; Patton, R. L.; Wilson, S. T. In *New Developments in Zeolite Science and Technology*; Lijima, A., Murakami, Y., Ward, J. W., Eds.; Kodanhsa: Tokyo, Japan, 1986; pp 103−112.

(4) Wilson, S. T.; Flanigen, E. M. In *Zeolite Synthesis*; Occelli, M. L., Robson, H. E., Eds.; ACS Symposium Series American Chemical Society: Washington, DC, 1989; pp 329−345.

(5) Lever, A. B. P. *Inorganic Electronic Spectroscopy*; Elsevier: The Netherlands, 1968; pp 249−305.

(6) Bordiga, S.; Ruzzoni, R.; Geobaldo, F.; Lamberti, C.; Giamello, E.; Zecchina, A.; Leofanti, G.; Petrini, G.; Tozzola, G.; Vlaic, G. *J. Catal.* **1996**, *158*, 486−501.

(7) Barrie, P. J.; Klinowski, J. *J. Phys. Chem.* **1989**, *93*, 5972−5974.

(8) Bertini, I.; Luchinat, C. In *Physical Methods*; Drago, R. S., Ed.; Sounders College Publishing: Philadelphia, 1977; pp 500−533.

(9) Goldfarb, D. *Zeolites* **1989**, *9*, 509−514.

(10) Canesson, L.; Boudeville, Y.; Tuel, A. *J. Am. Chem. Soc.* **1997**, *119*, 10754−10762.

(11) Reed, G. H.; Markham, D. In *Biological Magnetic Resonance*; Berliner, L. J., Reuben, J., Eds.; Plenum Press: New York, 1984; Vol. 6, pp 73−142.

(12) De Vos, D. E.; Weckhuysen, B. M.; Bein, T. *J. Am. Chem. Soc.* **1996**, *118*, 9615−9622.

(13) Mims, W. B. *Phys. Rev. B* **1972**, *5*, 2409−2419.

10.1021/ja990365n CCC: $18.00 
Published on Web 06/11/1999

nuclear double resonance (ENDOR)[16,17] techniques. The ESEEM technique allows measurements of weak superhyperfine couplings in solids.[15] In zeolites and related materials, it can be used to probe interactions between TM centers and framework $^{27}Al$[18,19] or $^{31}P$[20,21] as well as with adsorbate molecules.[22,23] Pulsed ENDOR, which is commonly applied through the Mims[24] or Davies[25] pulse sequences, is complementary to ESEEM, as it can generally measure larger hyperfine couplings, associated either with the central atom, as is the case of $^{55}Mn(II)$[26] and $^{57}Fe(III)$,[27] or with directly bound nuclei.[28]

So far, the majority of the EPR studies of Mn(II) in zeolites has been done using conventional X- and Q-band ($\nu_0 \approx 35$ GHz) spectrometers.[12,29,30] Moving to higher frequencies is highly advantageous for $S = {}^5/_2$ systems in orientationally disordered materials. This is due to the reduced effect of the ZFS[31,32] on the central $|-{}^1/_2\rangle \rightarrow |+{}^1/_2\rangle$ transition, which leads to improved resolution and, hence, to an easier interpretation of the spectrum.[33] In addition, at low temperatures, the larger difference in the Boltzmann population of the different $M_S$ levels is helpful in reducing the number of observed EPR transitions and in determining the sign of the ZFS interaction.[32,34] Moreover, in pulsed experiments, the spectrometer dead time is significantly reduced,[35] which is particularly helpful for TM detection, where the echo decay is inherently fast. High-field ENDOR benefits from the appreciably larger nuclear Zeeman interaction, which helps in resolving signals due to nuclei with similar gyromagnetic ratios ($\gamma$) (e.g., $^{23}Na$ and $^{27}Al$),[32] and improves the detection of low $\gamma$ nuclei with small hyperfine couplings.[36] In an earlier work we used high-field ENDOR to determine the characteristic hyperfine interaction of $^{57}Fe(III)$ in a zeolite T site, and measured its dipolar interaction with $^{23}Na^+$ cations in sodalite.[32] However, there are applications, for which high-field is not the best of choices; weak anisotropic hyperfine interactions are often better detected by ESEEM at lower fields where the nuclear modulation depth is stronger.[37] Hence, combining W- with X-band experiments is preferred for a systematic study in general and for Mn(II) centers in particular.

In this work, we present X-band ESEEM and W-band pulsed ENDOR measurements on $MnAlPO_4$-20, which crystallizes in the sodalite structure (Figure 1).[38] We report for the first time on a $^{31}P$ hyperfine coupling of $\sim$8 MHz, which provides direct evidence for framework substitution.

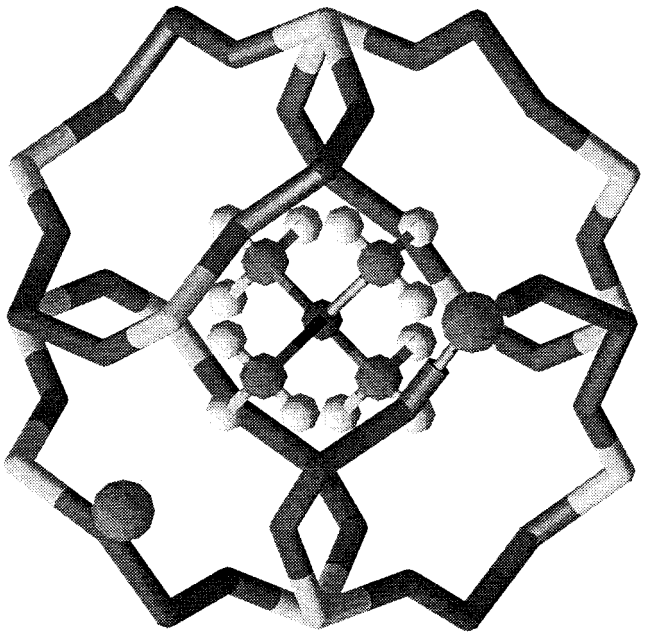

**Figure 1.** Structure of the $\beta$ cage in $AlPO_4$-20, viewed along the cubic unit cell direction, showing possible locations of manganese. The manganese and the TMA cations are designated by balls, and the aluminophosphate framework atoms are designated by cylinders. One manganese cation is substituted in a framework T site (3.14 Å from the next T site), whereas the other is in the middle of a six-ring, 1.11 Å above its plane (3.33 Å from the nearest T site).[38]

## Experimental Section

**Zeolite Synthesis.** The composition of the synthesis gel of the $MnAlPO_4$-20 sample was: $P_2O_5$:$Al_2O_3$:50$H_2O$:0.5$(TMA)_2O$:0.01MnO. The synthesis procedure, using tetramethyl ammonium (TMA) hydroxide as a templating agent, was similar to that given in earlier reports.[4,39] The manganese was introduced as a 25% water solution of $Mn(CH_3COO)_2 \cdot 4H_2O$, (Aldrich), and the white product was centrifuged and dried at 100 °C. The product was characterized by powder X-ray diffraction (XRD) using a Siemen D500 automated diffractometer. The XRD pattern was similar to that reported for sodalite.[40] The relative manganese content in the final product, determined by ICP, was Mn/Al = 0.007 by molar ratio. Similar MnSAPO-20 samples, with low silicon levels (Si/Al = 0.01−0.03) were prepared as well by using aqueous silica (Ludox HS-40, DuPont).

**EPR and Pulsed-EPR measurements.** CW X-band EPR spectra were recorded on a Varian E-12 spectrometer (9.3 GHz). The spectrum

(14) Kevan, L. In *Time Domain Electron Spin Resonance*; Kevan, L., Schwartz, R.N., Eds.; Wiley: New York, 1979; pp 279−341.
(15) Dikanov, S. A.; Tsvetkov, Y. D. *Electron Spin Echo Envelope Modulation Spectroscopy*; CRC Press: Boca Raton, FL, 1992; pp 359−389.
(16) Kurreck, H.; Kirste, B.; Lubitz, W. *Electron Nuclear Double Resonance Spectroscopy of Radicals in Solution*; VCH Publishers: New York, 1988; pp 7−77.
(17) Gemperle, C.; Schweiger, A. *Chem. Rev.* **1991**, *91*, 1491−1505.
(18) Matar, K.; Goldfarb, D. *J. Phys. Chem.* **1992**, *96*, 3100−3109.
(19) Samoilova, R. I.; Astashkin, A. V.; Dikanov, S. A.; Goldfarb, D.; Lunina, E. V. *Colloids Surf. A.* **1993**, *72*, 29−35.
(20) Yu, J. S.; Kurshev, V.; Kevan, L. *J. Chem. Phys.* **1994**, *98*, 10225−10228.
(21) Azuma, N.; Kevan, L. *J. Phys. Chem.* **1995**, *99*, 5083−5088.
(22) Kevan, L. *Acc. Chem. Res.* **1986**, *20*, 1−7.
(23) Pöppl, A.; Hartmann, M.; Kevan, L. *J. Phys. Chem.* **1995**, *99*, 17251−17258.
(24) Mims, W. B. *Proc. R. Soc. London* **1965**, *283*, 452−457.
(25) Davies, E. R. *Phys. Lett. A* **1974**, *47*, 1−2.
(26) Sturgeon, B. E.; Ball, J. A.; Randall, D. W.; Britt, R. D. *J. Phys. Chem.* **1994**, *98*, 12871−12883.
(27) Vardi, R.; Bernardo, M.; Thomann, H.; Strohmaier, K. G.; Vaughan, D. E. W.; Goldfarb, D. *J. Magn. Reson.* **1997**, *126*, 229−241.
(28) Telser, J.; Lee, H. I.; Smith, E. T.; Huang, H.; Brereton, P.; Adams, M. W. W.; Conover, R. C.; Johnson, M. K.; Hoffman, B. M. *App Magn. Reson.* **1998**, *14*, 305−321.
(29) Levi, Z.; Raitsimring, A. M.; Goldfarb, D. *J. Phys. Chem.* **1991**, *95*, 7830−7838.
(30) Olender, Z.; Goldfarb, D.; Batista, J. *J. Am. Chem. Soc.* **1993**, *115*, 1106−1114.
(31) Gaffney, B. J.; Silverstone H. In *Biological Magnetic Resonance, EMR of Paramagnetic Molecules*; Berliner, L. J., Reuben, J., Eds.; Plenum Press: New York, 1993; Vol. 13, pp 1−57.
(32) Goldfarb, D.; Bernardo, M.; Strohmaier, K. G.; Vaughan, D. E. W.; Thomann, H.; Poluektov, O. G.; Schmidt, J. *J. Am. Chem. Soc.* **1996**, *118*, 4665−4671.
(33) Bellew, B. F.; Halkides, C. J.; Gerfen, G. J.; Griffin, R. G.; Singel, D. J. *Biochemistry* **1996**, *35*, 12186−12193.
(34) Goldberg, D. P.; Telser, J.; Krzystek, J.; Montablan, A. G.; Brunel, L. C.; Barret, A. G. M.; Hoffman, B. M. *J. Am. Chem. Soc.* **1997**, *119*, 8722−8723.
(35) Prisner, T. F.; Un, S.; Griffin, R. G. *Isr. J. Chem.* **1992**, *32*, 357−363.
(36) Groenen, E. J. J.; Canters, G. W.; Nar, H.; Coremans, J. W. A.; Poluektov, O. G.; Messerschmidt, A. *J. Am. Chem. Soc.* **1996**, *118*, 12141−12153.
(37) Romanelli, M.; Kurshev, V.; Kevan, L. *App. Magn. Reson.* **1994**, *7*, 427−441.
(38) Lons, V. J.; Schultz, H. *Acta Crystallogr.* **1967**, *23*, 434−436.
(39) Arieli, D.; Vaughan, D. E. W.; Strohmaier, K. G.; Thomann, H.; Bernardo M.; Goldfarb, D. *Magn. Reson. Chem.*, in press.
(40) Treacy, M. M. J.; Higgins, J. B.; Ballmoos, V. R. *Zeolites* **1996**, *16*, 581.

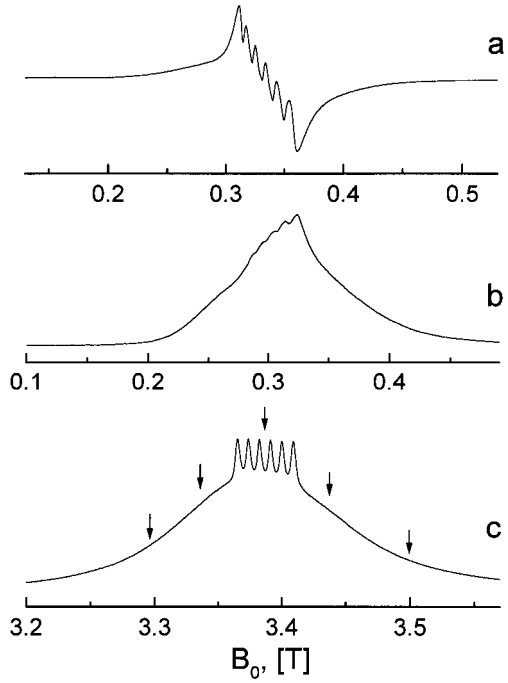


**Figure 2.** EPR spectra of $MnAlPO_4$-20 (a) CW-EPR spectrum (160 K), (b) X-band FS-ED spectrum (4.3 K, $\tau = 260$ ns), (c) W-band FS-ED spectrum (4.3 K, $\tau = 300$ ns). The arrows indicate field positions where $^1$H Mims-ENDOR spectra were measured.

was measured in the range 0−0.8 T with a typical modulation amplitude of 1 mT. The X-band pulsed experiments were carried out on a home-built spectrometer[41,42] at 8.5 GHz and temperatures of 2.4 or 4.3 K. Field sweep echo-detected (FS-ED) spectra were measured using the two-pulse echo sequence with $\pi/2$ and $\pi$ pulses of 20 and 40 ns, respectively. ESEEM spectra were obtained using the three-pulse sequence with $\pi/2$ pulses of 20 ns and the appropriate phase cycling.[43] The time domain waveforms were normalized to the maximum intensity, and the echo decay was removed by a polynomial fit. The resulting waveforms were convoluted with a sinebell function to remove artifacts due to the dead time and the background decay removal and with a Hanning window function for improved resolution. Zero-filling up to 1024 points was carried out, followed by Fourier transformation (FT) and magnitude mode calculations. W-band pulsed experiments (94.9 GHz) were carried out on a home-built spectrometer at 4.3 K.[44] The field was calibrated using the $^1$H ENDOR lines of a Cu(II)−histidine complex. The FS-ED spectrum was obtained using the two-pulse echo sequence with pulses of 40 and 60 ns, respectively. Mims-ENDOR experiments were recorded with $\pi/2$ pulse duration of 40 ns and an RF pulse length of 20 $\mu$s. Davies-ENDOR spectra were obtained with selective MW pulses where the $\pi$ and $\pi/2$ pulse lengths were 200 and 100 ns, respectively, and an RF pulse length of 9 $\mu$s. In this case it was necessary to use shorter RF pulses due to the relatively fast recovery of the inverted echo. The repetition rates were 1 and 0.5 kHz for the FS-ED EPR and ENDOR experiments, respectively.

## Results

The CW X-band EPR spectrum of MnAlPO-20 is shown in Figure 2a. As the condition $D \ll g\beta B_0$ holds, the spectrum is dominated by a resolved sextet corresponding to the $|-^1/_2, M_I\rangle \rightarrow |+^1/_2, M_I\rangle$, *central* transitions superimposed on the other $|M_S$,

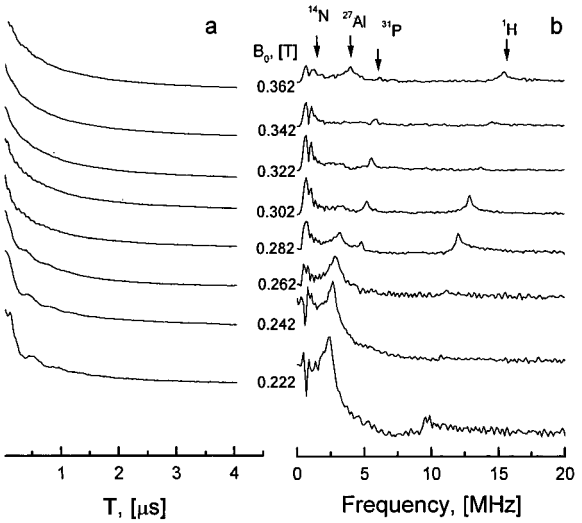


**Figure 3.** Field dependence of the X-band three-pulse ESEEM spectra (2.4 K, $\tau = 260$ ns) of $MnAlPO_4$-20 (a) time domain waveforms and (b) magnitude mode FT-ESEEM spectra.

$M_I\rangle \rightarrow |M_S \pm 1, M_I\rangle$ transitions.[11,45] Higher order effects of the ZFS are well evident by the increased splitting from low to high field and the appearance of forbidden transitions.[45,46] The X-band FS-ED spectrum, shown in Figure 2b, is poorly resolved and distorted due to the *nuclear modulation* effect.[47,48] The sharpening of the manganese hyperfine lines is very clear in the W-band spectrum, Figure 2c, and a $^{55}$Mn hyperfine coupling of 8.7 mT is easily determined from this spectrum. Similar spectra were exhibited by the MnSAPO-20 samples.

X-band ESEEM measurements were carried out across the EPR powder pattern, and the results are presented in Figure 3. Throughout the field range of the FS-ED spectra, modulations corresponding to the Larmor frequencies of $^{14}$N, $^{27}$Al, $^{31}$P, and $^1$H are observed, similar to the results obtained for Fe incorporated into $AlPO_4$-20.[39] Soaking the sample in $D_2O$ did not lead to a noticeable decrease in the $^1$H peak, indicating that the $^1$H modulations come primarily from TMA and not from water or OH ligand. The shallow modulation (Figure 3a) implies that the dipolar interactions with the $^{27}$Al nuclei ($I = ^5/_2$) are relatively weak.[49] The fast decay of the echo is due to spectral diffusion resulting form a relatively high Mn(II) content.

Figure 4a shows the field dependence of the W-band Mims ENDOR spectra in the $^{27}$Al and $^{31}$P regions. Peaks at the Larmor frequency of the two nuclei appear and a doublet with hyperfine splitting of ∼8 MHz, positioned symmetrically around the Larmor frequency of $^{31}$P is well resolved. This doublet appears at all fields where the central EPR transition has a significant contribution, and from the field dependence of the two lines a $\gamma$ value equal to that of $^{31}$P is extracted. The "fine" structure of the doublet components is a consequence of the *blind spots* effect.[17] This was confirmed by repeating the experiment for different $\tau$ values and by comparison with the corresponding Davies ENDOR spectrum, shown in Figure 4b, where the $^{31}$P doublet is clear and the lineshape is free from blind spots. The width of each component is ∼3 MHz, and a weak peak at the Larmor frequency of $^{27}$Al appears as well.

(41) Goldfarb, D.; Fauth, J. M.; Tor, Y.; Shanzer, A. *J. Am. Chem. Soc.* **1991**, *113*, 1941−1948.
(42) Shane, J. J.; Gromov, I.; Vega, S.; Goldfarb, D. *Rev. Sci. Instrum.* **1998**, *69*, 3357−3364.
(43) Fauth, J. M.; Schweiger, A.; Braunschweiler, L.; Forrer, J.; Ernst, R. R. *J. Magn. Reson.* **1986**, *66*, 74−85.
(44) Gromov, I.; Krymov, V.; Manikandan, P.; Arieli, D.; Goldfarb, D. *J. Magn. Reson.*, in press.
(45) Abragam, A.; Bleaney, B. *Electron Paramagnetic Resonance of Transition Ions*; Calderon Press: Oxford, 1970; pp 436−442.
(46) Meirovitch, E.; Poupko, R. *J. Chem. Phys.* **1978**, *82*, 1920−1925.
(47) Goldfarb, D.; Kevan, L. *J. Magn. Reson.* **1988**, *76*, 276−286.
(48) Schweiger, A. *Angew. Chem.* **1991**, *91*, 265−292.
(49) Subin, A. A.; Dikanov, S. A.; Parmon, V. N. *J. Magn. Reson.* **1981**, *42*, 474−487.

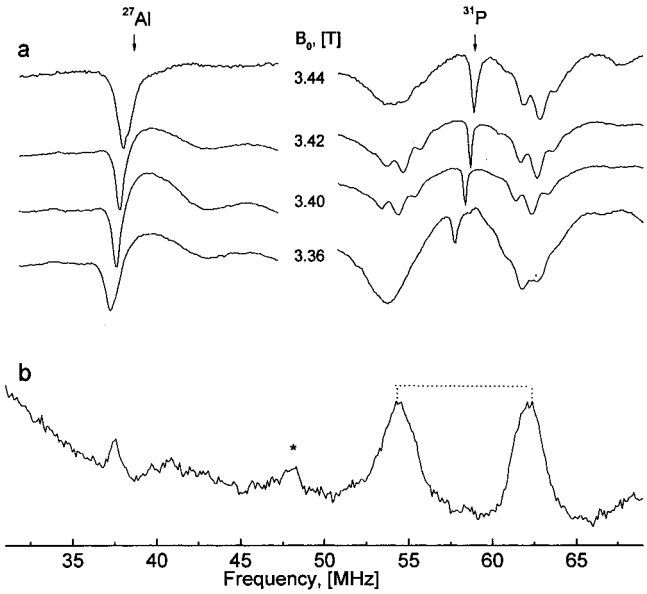


**Figure 4.** W-band ENDOR (4.3 K) spectra of $MnAlPO_4$-20, measured in the $^{27}Al$ and $^{31}P$ regions (a) Mims-ENDOR ($\tau = 400$ ns) measured at different field positions along the EPR spectrum, as indicated on the figure. The broad features near the $^{27}Al$ line are due to baseline distortions. (b) Davies ENDOR ($\tau = 400$ ns) measured at $B_0 = 3.4$ T. The doublet, mentioned in the text, is marked with dashed lines. The small line, marked with an asterisk, is due to $^1H$ harmonic.

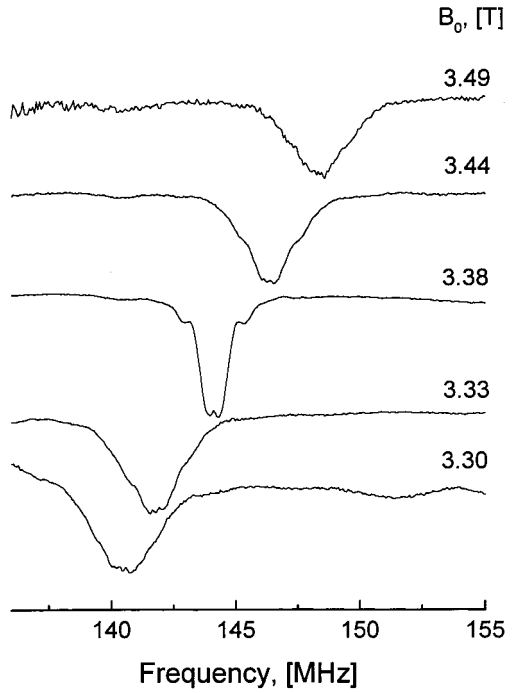


**Figure 5.** $^1H$ region of the W-band Mims ENDOR (4.3 K, $\tau = 500$ ns) spectra of $MnAlPO_4$-20 obtained at different field positions along the EPR spectrum.

Field-dependent W-band Mims ENDOR spectra in the $^1H$ region are shown in Figure 5 (the field positions are marked with arrows on the FS-ED spectrum in Figure 2c). In all of the spectra the center of the spectrum corresponds to the proton Larmor frequency, and a significant increase in the linewidth is apparent when measuring away from the central EPR transitions. In both $^{31}P$ and $^1H$ Mims ENDOR spectra the fine structure due to the blind spots becomes less resolved as the field at which the spectra are recorded shifts from the center of the EPR spectrum towards the edges, and the contribution of the $|-1/2, M_I\rangle \rightarrow |+1/2, M_I\rangle$ decreases. The ENDOR spectra of MnSAPO-20 (Si/Al = 0.03) showed features similar to those of $MnAlPO_4$-20. We were not able to measure the X-band $^{31}P$ ENDOR spectra due to the relatively weak and fast decaying echo.

## Discussion

While the X-band ESEEM results indicated that Mn(II) interacts via weak dipolar couplings with the framework nuclei, $^{31}P$ and $^{27}Al$, as well as with the template $^{14}N$ and $^1H$ nuclei, a strong interaction with framework $^{31}P$ is evident from the well resolved $^{31}P$ doublet in the W-band ENDOR spectra. The ENDOR frequencies of a $S = 5/2$ electronic spin system coupled to a $I = 1/2$ nucleus on a ligand subjected to the condition $D \ll g\beta B_0$ are[27]

$$\nu_{M_S}^{ENDOR} = [(M_S A_{zz} - \nu_I)^2 - M_S^2(A_{xz}^2 + A_{yz}^2)]^{1/2} \qquad (1)$$

where $A_{zz}$, $A_{xz}$, and $A_{yz}$ are the components of the hyperfine tensor in the laboratory frame and $\nu_I$ is the nucleus Larmor frequency. In eq 1 the third-order effects of the hyperfine and ZFS interactions are neglected. For a qualitative interpretation of the ENDOR spectrum this expression can be simplified by neglecting the pseudosecular parts of the hyperfine interaction which yields

$$\nu_{M_S}^{ENDOR} = |\nu_I - M_S A| \qquad (2)$$

where $A = A_{zz} = a_{iso} + a_\perp (3\cos^2\theta - 1)$, when the point−dipole approximation applies $a_\perp = \mu_0 g_e \beta_e g_n \beta_n / 4\pi h r^3$. $r$ is the electron-nuclear distance and $\theta$ is the angle between the electron-nuclear vector and the direction of the external magnetic field. Accordingly, for the case of $\nu_I > M_S A$, where all the $M_S$ levels are populated and excited by the microwave irradiation, a pair of ENDOR lines for each $|M_S|$, positioned symmetrically around $\nu_I$ should be resolved. The separation between the components of each doublet is $A$, $3A$, $5A$ for $M_S = \pm 1/2, \pm 3/2, \pm 5/2$ respectively. ENDOR features due to several values of $M_S$, if properly assigned, provide a self-consistent determination of $A$.

The lineshape of the $^{31}P$ doublet indicates that the hyperfine interaction is primarily *isotropic* and the anisotropic part is limited by the linewidth (3 MHz). On the basis of the relative populations of the different $M_S$ levels at 4.3 K,[50] the symmetric doublet observed is assigned to $M_S = \pm 1/2$, from which $|a_{iso}| \approx 8$ MHz is determined. At this temperature the $M_S = -5/2$ and $M_S = -3/2$ levels are populated and observed in the FS-ED EPR spectrum, and therefore, two more ENDOR lines are expected. Their positions depend on the sign of $a_{iso}$; for $a_{iso} < 0$ and $B_0 = 3.39$ T they should appear at 47 and 39 MHz for the $M_S = -3/2$ and $M_S = -5/2$ respectively, whereas for $a_{iso} > 0$, the positions are 70 and 78 MHz, respectively. Unfortunately, none of the above lines has been observed. This, however, is not surprising since the inhomogeneous linewidth of these peaks, determined by the anisotropic component of the hyperfine interaction, is expected to be 3 and 5 times larger than that of the $\pm 1/2$ doublet, thus rendering their detection more difficult. The observation of these lines would have determined the sign of $a_{iso}$, from which the mechanism responsible for this interaction could be obtained.

The appearance of a relatively large isotropic $^{31}P$ hyperfine coupling, which is a "through bonds" interaction, and the

(50) The relative populations of a $S = 5/2$ with a dominant Zeeman interaction at 94.9 GHz are 1: 0.35: 0.12: 0.04: 0.01: 0.005 for $|-5/2\rangle$: $|-3/2\rangle$:$|-1/2\rangle$:$|+1/2\rangle$:$|+3/2\rangle$:$|+5/2\rangle$.

**Table 1.** Calculated $^{31}P$ and $^{27}Al$ Dipolar Interaction[a] for Framework and Nonframework Mn

| configuration | no. of $^{31}P$ neighbors | $r_{P-Mn}$ [Å] | $a_\perp$, $^{31}P$ [MHz] | no. of $^{27}Al$ neighbors | $r_{Al-Mn}$ [Å] | $a_\perp$, $^{27}Al$ [MHz] |
|---|---|---|---|---|---|---|
| Mn substitutes Al | 4 | 3.14 | 1.03 | 2 | 4.44 | 0.24 |
| | | | | 8 | 5.44 | 0.13 |
| Mn substitutes P | 2 | 4.44 | 0.36 | 4 | 3.14 | 0.66 |
| | 8 | 5.44 | 0.20 | | | |
| extraframework Mn | 3 | 3.33 | 0.86 | 3 | 3.33 | 0.56 |

[a] The point dipole approximation was applied.

absence of such an $^{27}Al$ coupling provide a direct evidence for framework substitution of Mn in an Al site. Furthermore, the former shows that the bonding has a significant covalent contribution. In a framework site the Mn(II) is surrounded by four $^{31}P$ at a distance of 3.14 Å, two $^{27}Al$ nuclei at a distance of 4.44 Å, and eight $^{27}Al$ nuclei at a distance of 5.44 Å. In contrast, Mn(II) located in an extraframework site will be situated close to the negatively charged $^{27}Al$ (see Table 1), and considering the structure of sodalite, similar couplings to $^{31}P$ and $^{27}Al$ are expected.

The dipolar components of the $^{31}P$ and $^{27}Al$ hyperfine interaction, $a_\perp$, calculated for different Mn(II) locations are listed in Table 1. A potential extraframework Mn(II) site is the cation position in sodalite,[38] situated at the center of the 6-ring, 1.11 Å above its plane. The small calculated values of $a_\perp$ confirm that the main contribution to the hyperfine splitting is indeed isotropic. In the case of framework substitution for $^{27}Al$, the largest dipolar interaction, obtained for $r_{P-Mn} = 3.14$ Å, is 1.03 MHz; thus, the total width expected for each of the $M_S = \pm 1/2$ doublet is about 1.5 MHz.[51] This value is only one-half of the experimental linewidth of the doublet, extracted from the Davies spectrum (Figure 4b). We attribute the residual broadening to some distribution in the $^{31}P$ hyperfine parameters which could be introduced by specific interactions with the template molecules as observed in the case of the ZFS interaction in $FeAlPO_4$-20.[39]

The isotropic hyperfine interaction reflects the fractional spin density at the nucleus. One unpaired electron ($S = 1/2$) in a 3s orbital of $^{31}P$ gives $a_{iso} = 13306$ MHz.[52] Thus, 8 MHz corresponds to a spin density of 0.06%. This number is about one-half of the experimental value reported for $^{31}P$ in DAF-2, a microporous cobalt phosphate in which all phosphorous atoms are surrounded by four Co atoms. The latter value was obtained per Co−O−P bond from the $^{31}P$ paramagnetic shift induced by Co(II) ($S = 3/2$).[10]

The width of the $^1H$ ENDOR spectrum, recorded at fields where the $|-1/2, M_I\rangle \rightarrow |+1/2, M_I\rangle$ transitions has significant contribution, is rather narrow, 3 MHz, which is consistent with interaction with template protons rather than water or hydroxyl ligands. The latter should lead to splitting of ≈5 MHz.[51] The spectrum becomes broader at magnetic fields where the contribution of the central transition decreases and that of the other transitions increases. Again, this is attributed to the increased width of the powder pattern of the ENDOR lines corresponding to the $M_S = -3/2, -5/2$ manifolds (eq 2).

The hyperfine coupling of the $^{55}Mn$, 8.7 mT, was easily determined from the W-band FS-ED spectrum. This value is similar to a value previously reported for Mn(II) in Zeolite A which was assigned to tetrahedral coordination, based on the correlation between the value of the hyperfine coupling and the change in the coordination number of Mn(II).[12] This value, however, is also close to that of Mn(II) in an octahedral symmetry (for example, octahedral Mn(II) in MgO[45]), and therefore cannot be used as a reliable evidence for framework substitution. The Mn(II) hyperfine coupling in $MnAlPO_4$-5 and MnSAPO-44 were 9.0 and 8.5 mT, respectively,[29,30] and upon calcination and dehydration the latter decreased to 6.5 mT. This reduction was attributed to a change from octahedral to tetrahedral coordination of the Mn(II) due to the loss of coordinated water molecules. This change was also associated with the low stability of MnSAPO-44 towards hydrolysis, that led to sample decomposition after rehydration.

The advantages of high-field EPR and high-field ENDOR are very well demonstrated in this work and allowed us to observe for the first time the $^{31}P$ hyperfine coupling in metal-substituted aluminophosphate molecular sieves. This can be further applied to other frameworks and thus provide information on the effect of the structure on the bonding characteristics. The $^{31}P$ doublet was not detected by X-band ESEEM due to the width of the lines (∼3 MHz), which results in a very fast decay of the nuclear modulations (within the spectrometer dead time). It may be possible to observe, at least one of the doublet component at C-band ESEEM (∼6 GHz), where line-narrowing of the lower frequency component should occur, due to matching of the nuclear Zeeman and the hyperfine interactions.[53] Nonetheless, caution should be exercised when interpreting ESEEM data without complementary ENDOR results. At X-band frequencies the ENDOR spectrum should exhibit a doublet at ∼1.5 and ∼9.5 MHz. Taking into account their linewidth, it is expected that the low frequency component will be extremely hard to observe.

## Conclusion

The incorporation of low levels of Mn(II) into $AlPO_4$-20 results in a single Mn(II) species, situated in a framework site, and exhibiting a $^{55}Mn$ hyperfine coupling of 8.7 mT. The presence of a $^{31}P$ doublet with $|a_{iso}| \approx 8$ MHz in the W-band ENDOR spectrum, combined with the absence of such a doublet due to $^{27}Al$ provide a unique and direct proof for framework substitution of Mn(II) for Al.

This work demonstrates the potential applications of W-band ENDOR in the study of high-spin transition metal ions. The appreciably higher sensitivity, combined with the larger nuclear Zeeman interaction and the reduced weight of second- and third-order broadening effects, significantly improves the resolution of the EPR and ENDOR spectra.

**Acknowledgment.** This research was supported by a grant from the United States−Israel Binational Science Foundation (BSF), Jerusalem, Israel.

JA990365N

(51) Tan, X.; Bernardo, M.; Thomann, H.; Scholes, C. P. *J. Chem. Phys.* **1992**, *98*, 5147−5157.

(52) Atherton, N. M. *Principles of Electron Spin Resonance*; Ellis Horwood, 1993; p 87.

(53) Grefen, G. J.; Bellew, B. F.; Singel D. J. *Chem. Phys. Lett.* **1991**, *180*, 490−496.